

Computer Simulation and Statistical Theory of a Screened-Coulomb 2–2 Electrolyte Solution Model

SJUR A. ROGDE^a and BJØRN HAFSKJOLD^{b*}

^a Kjemisk Institutt, Universitetet i Bergen, N-5014 Bergen-Universitetet, Norway and ^b Institutt for uorganisk kjemi, Norges tekniske høgskole, Universitetet i Trondheim, N-7034 Trondheim-NTH, Norway

Thermodynamic and structural properties of a screened-Coulomb charged hard-sphere model are computed by means of statistical theories and Monte Carlo (MC) computer simulations. The model represents aqueous solutions of 2–2 electrolytes at 25 °C. The theories in consideration are the mean spherical approximation (MSA) and some approximations that are closely related to the MSA, the hypernetted chain (HNC) equation and a new modification of the Percus-Yevick (PYRL) equation. The theories are discussed in terms of the exact Monte Carlo results. Salt concentrations cover the range from 0.0001 M to 3 M. We find that HNC and PYRL are in good agreement with MC results over the entire concentration range, the EXP agrees at low concentrations, whereas the other theories are rather poor. The HNC and PYRL are found to predict the density of triple-ion clusters (+ – + and – + –) in good agreement with MC results.

1. INTRODUCTION

During the last couple of decades there has been significant progress in the theory of electrolyte solutions. The main reason is the development of computer-simulation methods because they yield properties of model systems in a formally exact way. Simulations are often called computer “experiments” due to their similarity with laboratory experiments. Approximate statistical theories, which are generally less laborious than simulations, can be discussed in terms of the exact results.

The long range of Coulomb interactions gives rise to special methodological problems in computer

simulations of electrolyte solutions and molten salts. This was observed by Krogh-Moe *et al.* as a drift of the internal energy of a LiCl model towards unreasonably low values during the computation.¹ Woodcock and Singer² found that this drift did not occur when they computed the energy by the Ewald method³ instead of the Evjen (or minimum image) method⁴ that Krogh-Moe and coworkers had used. Valleau and Whittington⁵ have given a discussion of these methodological problems and the possible erroneous effect of periodic boundary conditions as compared to a real, uniform fluid.

In an earlier paper,⁶ we discussed a close structural similarity between Coulombic and Yukawa (screened Coulombic) systems, which was used in a perturbation theory of the former. The Yukawa interaction was made so short-ranged that the problems with energy computation were not encountered and simulations could be carried out as usual for simple fluids.⁷ Because of the structural similarity, the perturbation from Yukawa to Coulomb potential is small and the theory presumably accurate. Properties of the Coulombic system could thus be obtained in a way circumventing the methodological problems of a direct simulation.

Apart from its relation to Coulombic systems, the Yukawa system is of interest to us also because it is so well-suited for studies of various consequences of the range of the potential.⁶

In the present paper, we focus on the thermodynamic and structural properties of a model that we have called the RPMY. It consists of charged hard spheres of diameter R . The pair potential is given by (1.1), where e_i is the charge on ion i and z a screening parameter, which determines the range of the potential. The ions are immersed in

* Previously Bjørn Larsen (changed name since June, 1980).

$$u_{ij}(r) = \begin{cases} \infty & \text{for } r < R \\ \frac{e_i e_j}{\epsilon r} \cdot e^{-z(r-R)/R} & \text{for } r > R \end{cases} \quad (1.1)$$

a medium represented by its dielectric constant ϵ , and they are charge symmetric, *i.e.* $e_+ = -e_-$.

In the limiting case $z \rightarrow 0$, the RPMY becomes identical to the so-called restricted primitive model (RPM), which is known to be a realistic model for electrolyte solutions and molten salts.⁸ We anticipate from the observed relation between the two models⁶ that the structural short-range properties of the RPMY are very similar to those of the RPM. The present work thus complements some recent studies on the structure of electrolyte models.⁹⁻¹¹ Further application of the perturbation theory for the RPM in terms of the RPMY reference system will be discussed in a future paper.

The thermodynamic states of the RPM and RPMY are determined by two variables, which in the canonical ensemble are conveniently chosen to be a reduced inverse temperature, β^* , and a reduced number density, ρ^* . These variables are defined by eqns. (1.2) and (1.3), where k is Boltzmann's constant,

$$\beta^* = e^2 / (ekTR) \quad (1.2)$$

$$\rho^* = NR^3/V \quad (1.3)$$

T the absolute temperature, N the total number of ions, and V the volume of the system. There are N_+ cations and N_- anions, subject to the electroneutrality condition $N_+ = N_- = N/2$. The RPMY is also determined by the screening parameter z . In the present work, the values of ρ^* and β^* were chosen typical for aqueous 2-2 electrolytes at 25 °C in the concentration range 0.0001 - 3 M.

Three largely analytic theories, the mean spherical approximation (MSA),¹² the EXP approximation of Andersen and Chandler,¹³ and the truncated Γ_2 approximation (TF2A),¹⁴ are described in Section 2. The hyper-netted chain (HNC) and Percus-Yevick (PY) equations are given in Section 3. We also discuss a modification of the PY equation due to Allnatt (PYA)¹⁵ and derive a new version of it, which we show is comparable in accuracy with the HNC. These equations must be solved by numerical methods, which are outlined in Section 3.

The Monte Carlo (MC) computer simulations are described in Section 4. In Section 5, we discuss the internal energy of the RPMY and the accuracy of the different theories in light of the MC results. Our main conclusion is that both HNC and PYRL are within 13% of the MC results over the entire concentration range, and they are within the statistical uncertainties of the MC values at the highest and lowest concentrations. The other theories are, in general, rather poor, with exception of the EXP at low concentrations.

The radial distribution functions are discussed in Section 6. We find there too, that the HNC and PYRL are most accurate and generally in good agreement with the MC results. Our results show that the tendency of triple-ion formation in the RPMY at intermediate concentrations is well-described by the HNC equation, which does not agree with what Rosky *et al.* have found in a recent study of a charged soft-sphere model.¹¹

2. APPROXIMATIONS

Mean spherical approximation. A set of approximations to the thermodynamic and structural properties of the RPMY can be obtained from their cluster expansions by neglecting all but the simplest terms. One such approximation is the mean spherical approximation (MSA), obtained by retaining only the leading contribution to the direct correlation function, eqn. (2.1), and combining this approximation with the exact relation (2.2) through

$$c_{ij}^{\text{MSA}}(r) = -\beta u_{ij}(r) \quad \text{for } r > R, \quad (2.1)$$

$$g_{ij}(r) = 0 \quad \text{for } r < R \quad (2.2)$$

the Ornstein - Zernike (OZ) equation. In eqn. (2.1), β^{-1} equals the product of Boltzmann's constant and the absolute temperature, and $g_{ij}(r)$ in eqn. (2.2) is the radial distribution function (rdf). Eqns. (2.1), (2.2), and the OZ equation form a closed set of equations, the solution to which is given as $c_{ij}(r)$ for $r < R$ and $g_{ij}(r)$ for $r > R$. The thermodynamic properties can then be computed from the correlation functions *via* one of the three routes; the energy equation, pressure equation or compressibility equation.

The MSA is of interest to us for two reasons. Firstly, it is a well-defined and self-contained approximation that may be considered an extension to the Debye-Hückel theory in that the ion's cores

are taken into account. (In the limit $R \rightarrow 0$, the MSA becomes identical to the Debye-Hückel theory.) Thus, in terms of the screening of the potential of average force, the MSA accounts for the hard-sphere screening in addition to the well-known Debye screening, and to some extent also for the combined effects of these elements. Secondly, the solution of the MSA is an important building block in more sophisticated approximations. Indeed, the cluster expansions for the properties of the RPMY may be renormalized and expressed in terms of the same functionals that appear in the solution of the MSA like it may be expressed in terms of the functionals that appear in the Debye-Hückel theory.

Waisman¹² has solved the MSA for the RPMY and expressed the internal energy as obtained from the energy equation in terms of a quartic equation for $w = 2U/NkT\beta^*$; eqn. (2.3), where $x = \rho^*\beta^*$

$$[1 + w(1 - e^{-z})/2z]^4 = -w(z - w/2e^z)/2\pi x \quad (2.3)$$

$= (eR)^2 \rho / ekT$. This equation is easily solved numerically with the Newton-Raphson method, and results for U/NkT are shown in Table 1.

The MSA rdf is given by eqns. (2.2) and (2.4).

$$g_{ij}^{\text{MSA}}(r) = g^{\text{HS}}(r) + (-1)^{i+j}C(r) \text{ for } r > R \quad (2.4)$$

Here, $C(r)$ is the so-called chain function,¹⁶ which can be expressed as the sum of diagrams of a certain topology in the cluster expansion of the exact rdf. The term $g^{\text{HS}}(r)$ is the rdf of hard spheres as given by the Percus-Yevick (PY) equation.¹⁷ The chain function $C(r)$ can be computed from Waisman's solution for the direct correlation function, eqn. (2.5)

$$c_{ij}^{\text{MSA}}(r) = c^{\text{HS}}(r) + (-1)^{i+j}\beta^*w \left[\frac{1 - e^{-zr}}{zr} + w \frac{\cosh(zr) - 1}{2z^2 e^z} \right] \text{ for } r < R \quad (2.5)$$

in combination with eqn. (2.1) and the OZ equation. The term $c^{\text{HS}}(r)$ is the direct correlation function for hard spheres as given by the PY equation.¹⁷ We shall present the MSA rdfs graphically for some thermodynamic states of the RPMY in Section 6.

The EXP-approximation of Andersen and Chandler¹³ is given by eqn. (2.6) and is readily computed from the solution for $C(r)$ from the MSA. The $g^{\text{HS}}(r)$ in eqn. (2.6) is the exact hard-sphere rdf.

$$g_{ij}^{\text{EXP}}(r) = g^{\text{HS}}(r) \exp[(-1)^{i+j}C(r)] \quad (2.6)$$

We have used the PY approximation for $g^{\text{HS}}(r)$, however, which makes little numerical difference for the hard-sphere densities we shall discuss in this paper. Some EXP rdfs for the RPMY are shown graphically in Section 6.

We have also computed the internal energy, U/NkT , from $g_{ij}^{\text{EXP}}(r)$ and the energy equation (2.7). Here, $g_D(r)$ is defined by eqn. (2.8). Numerical results are shown in Table 1.

$$\begin{aligned} \frac{U}{NkT} &= \frac{2\pi V}{NkT} \sum_{i,j=1}^{\infty} \rho_i \rho_j \int_0^{\infty} u_{ij}(r) g_{ij}(r) r^2 dr \\ &= 2\pi x e^z \int_1^{\infty} e^{-zr} r g_D(r) dr \end{aligned} \quad (2.7)$$

$$g_D(r) = \frac{1}{2}[g_{11}(r) - g_{12}(r)] \quad (2.8)$$

The truncated $\Gamma 2$ approximation ($\Gamma 2A$) is obtained by adding one term, eqn. (2.9), to the MSA Helmholtz' free energy per particle.¹⁴ The factor $g_1^{\text{HS}}(r)$ is the coefficient of the linear term in the density expansion of $g^{\text{HS}}(r)$. The $\Gamma 2A$ internal energy is then given by

$$s_{2,0} = -\pi \rho^{*2} \int_1^2 g_1^{\text{HS}}(r) C^2(r) r^2 dr \quad (2.9)$$

$$\left(\frac{U}{NkT} \right)_{\Gamma 2A} = \left(\frac{U}{NkT} \right)_{\text{MSA,E}} + \beta^* \frac{\partial s_{2,0}}{\partial \beta^*} \quad (2.10)$$

where subscript "MSA,E" denotes a quantity obtained from the energy equation in the MSA. The integral in eqn. (2.9) and the derivative in eqn. (2.10) have been computed numerically and results for the internal energy are given in Table 1.

The $\Gamma 2A$ has proved to be a very useful approximation for the thermodynamic properties of the hard-sphere Coulombic system,^{14,18} and it seems worthwhile to examine it also for the Yukawa system. However, the $\Gamma 2A$ is known to be inaccurate in the ρ^* , β^* -regime we investigate here because it lacks an important contribution, ΔB_2 , from the second ionic virial coefficient.^{14,19} This contribution can be computed numerically and added to the $\Gamma 2A$, resulting in the so-called $\Gamma 2AUB_2$.¹⁴ The MSA also lacks this contribution, whereas the EXP approximation incorporates the complete second ionic virial coefficient. The numerical difference between the $\Gamma 2A$ and the MSA is very small at low densities because of the

Table 1. Internal energy for the RPMY.

ρ^*	$c[\text{mol/l}]^a$	β^*	z	$n \times 10^{-5}{}^b$	$-U/NkT$						
					MC	MSA	$\Gamma 2A$	$\Gamma 2AUB_2$	EXP	HNC	PYRL
2.685×10^{-1}	3	2.2388	2	8	$1.051 \pm .010$	0.930	1.033	1.033	1.465	1.045	1.047
1.787×10^{-1}	2	2.3850	2	9	$0.918 \pm .007$	0.820	0.887	0.887	1.224	0.918	0.919
8.961×10^{-2}	1	2.6803	2	9	$0.752 \pm .010$	0.642	0.673	0.673	0.972	0.754	0.752
4.960×10^{-2}	0.56	3.6391	1	8	$1.088 \pm .010$	0.931	0.947	0.947	1.478	1.082	1.074
3.549×10^{-2}	0.4	3.7585	1	8	$1.003 \pm .011$	0.811	0.822	0.822	1.368	0.989	0.978
2.210×10^{-2}	0.25	3.9415	1	10	$0.888 \pm .011$	0.653	0.659	0.661	1.225	0.867	0.852
8.839×10^{-3}	0.1	4.3577	1	40	$0.708 \pm .006$	0.401	0.402	0.435	0.979	0.673	0.650
5.590×10^{-3}	0.06265	4.5858	1	40	$0.623 \pm .006$	0.304	0.305	0.376	0.860	0.589	0.566
2.231×10^{-3}	0.025	5.0618	1	40	$0.49 \pm .01$	0.163	0.163	0.329	0.634	0.446	0.426
8.924×10^{-4}	0.01	5.4991	1	40	$0.346 \pm .021$	0.081	0.081	0.288	0.422	0.318	0.307
4.461×10^{-4}	0.005	5.7948	1	40	$0.250 \pm .010$	0.046	0.046	0.232	0.291	0.235	0.229
2.231×10^{-4}	0.0025	6.0385	1	40	$0.175 \pm .018$	0.025	0.025	0.165	0.188	0.162	0.160
8.924×10^{-5}	0.001	6.2888	1	40	$0.095 \pm .014$	0.011	0.011	0.092	0.098	0.090	0.089
3.570×10^{-5}	0.0004	6.4640	1	40	$0.038 \pm .012$	0.005	0.005	0.045	0.046	0.045	0.045
8.924×10^{-6}	0.0001	6.6287	1	40	$0.012 \pm .005$	0.001	0.001	0.013	0.015	0.013	0.013

^a These concentrations are approximate values. The exact values are given by $c = 11.2059\rho^*$, assuming $R = 0.42 \text{ nm}$. ^b n is the number of configurations generated in each run.

factor ρ^{*2} in eqn. (2.9).

The $\Gamma 2A$ has no obvious analogue at the correlation-function level. The $\Gamma 2$ approximation, which is similar to the $\Gamma 2A$ except the $g_1^{\text{HS}}(r)$ of eqn. (2.9) is replaced by the complete $g^{\text{HS}}(r)$, does have such an analogue, however. Stell¹⁶ and Sun²⁰ have given diagrammatic expressions for it, and they have derived some simpler, analytic expressions appropriate for the low-density regime we consider here. These are eqns. (2.11) and (2.12); eqn. (2.11) was

$$g_{ij}^{\text{LIN}}(r) = g^{\text{HS}}(r)[1 + (-1)^{i+j}C(r)] \quad (2.11)$$

$$g_{ij}^{\text{SQ}}(r) = g^{\text{HS}}(r)[1 + (-1)^{i+j}C(r) + \frac{1}{2}C^2(r)]. \quad (2.12)$$

originally derived on a different basis by Verlet and Weis.²¹ Although none of these rdf's yield the $\Gamma 2A$ thermodynamics, they may in some sense be considered $\Gamma 2A$ analogues. Two remarks are relevant to the ρ^* , β^* -regime discussed here. First, LIN and MSA are not very different because $g^{\text{HS}}(r)$ is close to unity at these low densities. Second, SQ is not necessarily more accurate than LIN despite the fact that it includes the additional quadratic term, because $|C(r)|$ is much greater than unity for some values of r . We recognize, incidentally, LIN and SQ as truncated Taylor expansions of the EXP

approximation. Because of their symmetry properties, $g_{ij}^{\text{LIN}}(r)$ and $g_{ij}^{\text{SQ}}(r)$ yield the same thermodynamics by the energy equation, but they differ in the pressure and compressibility equations. Some examples of LIN and SQ are shown in Section 6.

If the theory is not thermodynamically self-consistent, the three different routes from the correlation functions will yield different sets of thermodynamic properties. To illustrate this, we have computed the excess compressibility factor, $\Delta PV/NkT$ (relative to the hard-sphere compressibility factor), in the MSA according to the three routes. The excess compressibility factor is a measure of the effective cohesion of the system. The lack of self-consistency may be used as a criterion for the validity of the theory. Waisman¹² has shown relation (2.12) and from the pressure equation we

$$\left(\frac{\Delta PV}{NkT}\right)_{\text{MSA,E}} = \frac{1}{2\rho^*} \left[x \cdot w(x) - \int_0^x w(x') dx' \right] \quad (2.12)$$

have⁶ eqn. (2.13), where p^2 and q^2 are given by eqns. (2.14) and (2.15). The excess compressibility factor as obtained from the compressibility equation is always zero in the MSA for the RPMY.

$$\left(\frac{\Delta PV}{NkT}\right)_{\text{MSA,P}} = \left(\frac{U}{3NkT}\right)_{\text{MSA,E}} \times \frac{z^2 + 2(1+q)z + 2(p^2 + q)}{z^2 + 2qz + 2p^2 - 2p^2 e^{-z}} \quad (2.13)$$

$$p^2 = -\pi\rho^*g_D(R+) = \frac{\pi\kappa[1 + w(1 - e^{-z})/2z]^2}{2z} \quad (2.14)$$

$$q^2 = p^2 + z^2/4 \quad (2.15)$$

Numerical results for the MSA,E and MSA,P estimates are compared with other theoretical predictions and Monte Carlo results in Table 2.

3. HNC AND PY INTEGRAL EQUATIONS

Analysis of the cluster expansion of the rdf leads to the relation²² (3.1), where $\gamma_{ij}(r) \equiv h_{ij}(r) - c_{ij}(r)$ ($h_{ij}(r) = g_{ij}(r) - 1$) is the sum of series diagrams and $B_{ij}(r)$ is the sum of bridge diagrams.

$$g_{ij}(r) = \exp[-\beta u_{ij}(r) + \gamma_{ij}(r) + B_{ij}(r)] \quad (3.1)$$

The hyper-netted chain (HNC) approximation is made by neglecting $B_{ij}(r)$; eqn. (3.2). In combination with the OZ equation, eqn. (3.3), it forms a complete

$$g_{ij}^{\text{HNC}}(r) = \exp[-\beta u_{ij}(r) + \gamma_{ij}(r)]. \quad (3.2)$$

$$\gamma_{ij}(r) = \sum_k \rho_k \int h_{ik}(r') c_{kj}(|r-r'|) dr', \quad (3.3)$$

set of integral equations that can be solved for $g_{ij}(r)$ and $c_{ij}(r)$. In the present case, we again make use of the exact relation (2.2), and the unknowns are $g_{ij}(r)$ for $r > R$ and $c_{ij}(r)$ for all r .

In general, the HNC equation must be solved numerically and we have employed the method described by Larsen²³ with some minor modifications that will be described below.

Another frequently used approximation is the Percus-Yevick (PY) approximation,²⁴ which may be derived from eqn. (3.1) by first neglecting $B_{ij}(r)$ and then linearizing with respect to $\gamma_{ij}(r)$; eqn. (3.4). For simple fluids, it turns out that the two approximations made here to some extent cancel

$$g_{ij}^{\text{PY}}(r) = \exp[-\beta u_{ij}(r)] \times [1 + \gamma_{ij}(r)]. \quad (3.4)$$

one another and that the PY is actually superior to the HNC. Moreover, $\gamma_{ij}(r)$ is generally small for these fluids. Rasaiah and Friedman²⁵ found the PY to be very poor for electrolyte solutions, where the linearization seems to be too drastic an approximation to make the errors cancel. This is in agreement with the expectation that $B_{ij}(r)$ is small compared to $\ln g_{ij}(r)$, whereas $\gamma_{ij}(r)$ is roughly $\beta u_{ij}(r)$ and may be quite large for $r \gtrsim R$ for ionic systems.

This problem was recognized by Allnatt,¹⁵ who suggested a PY-like approximation in terms of a renormalized $\gamma(r)$. His approach was based on a splitting of the pair potential into a short-range part $u_{ij}^o(r)$ and a long-range part $\Delta u_{ij}(r)$. Because this idea is relevant to a similar approximation we shall develop and discuss in this paper, we shall briefly describe the arguments leading to Allnatt's PY-approximation.

Taking $\Delta u_{ij}(r)$ to be Coulombic for all r , the cluster expansion for $g_{ij}(r)$ may be rearranged according to Mayer's renormalization,²⁶ and the $\Delta u_{ij}(r)$ bonds eliminated in favor of the Debye chain sum (3.5). The parameter κ is the inverse Debye screening length. Introducing $q_{ij}(r)$ into eqn. (3.1) leads to eqn. (3.6), where $\tau_{ij}(r)$ is given by eqn. (3.7).

$$q_{ij}(r) = (-1)^{i+j} \frac{e^2}{\epsilon kT} \cdot \frac{e^{-\kappa r}}{r} \quad (3.5)$$

$$g_{ij}(r) = \exp[-\beta u_{ij}^o(r) + q_{ij}(r) + \tau_{ij}(r) + B_{ij}(r)] \quad (3.6)$$

$$\tau_{ij}(r) \stackrel{\text{def}}{=} h_{ij}(r) - c_{ij}(r) - \beta \Delta u_{ij}(r) - q_{ij}(r) \quad (3.7)$$

From eqn. (3.7) we see that $\tau_{ij}(r)$, in contrast to $\gamma_{ij}(r)$, is relatively small because the two dominant terms, $c_{ij}(r)$ and $\beta \Delta u_{ij}(r)$ almost cancel. Neglecting $B_{ij}(r)$ leads to the HNC equation, and Allnatt arrived at his PY-type approximation by an additional linearization with respect to $\tau_{ij}(r)$; eqn. (3.8).

$$g_{ij}^{\text{PY}^\Lambda}(r) = \exp[-\beta u_{ij}^o(r) + q_{ij}(r)] [1 + \tau_{ij}(r)] \quad (3.8)$$

Rasaiah and Friedman²⁵ found that the PYA is indeed substantially better than the PY, although not as accurate as the HNC when applied to 2-2 electrolyte solutions. Apparently, linearization of $\exp[\tau_{ij}(r)]$ is also too crude an approximation for these systems. It can also be shown that PYA approaches the MSA asymptotically as $\kappa \rightarrow \infty$.¹⁵

We shall use Allnatt's idea, but make a different choice for $\Delta u_{ij}(r)$ for $r < R$. Specifically, we shall make

the same choice as in the optimized random phase approximation of Andersen and Chandler,¹³ which leads us to the exact relation (3.9), where $\tau'_{ij}(r)$ is given by eqn. (3.10). Eqn. (3.9) is another renormalized version of eqn. (3.1). Neglecting $B_{ij}(r)$ leads to the same HNC equation as before, and linearizing with respect to $\tau'_{ij}(r)$ leads to a new PY-type approximation that we shall call the PYRL; eqn. (3.11).

$$g_{ij}(r) = \exp[-\beta u_{ij}^0(r) + C_{ij}(r) + \tau'_{ij}(r) + B_{ij}(r)] \quad (3.9)$$

$$\tau'_{ij}(r) \stackrel{\text{def}}{=} h_{ij}(r) - c_{ij}(r) - \beta \Delta u_{ij}(r) - C_{ij}(r) \quad (3.10)$$

$$g_{ij}^{\text{PYRL}}(r) = \exp[-\beta u_{ij}^0(r) + C_{ij}(r)][1 + \tau'_{ij}(r)] \quad (3.11)$$

Analysis of eqns. (3.10) and (3.11) leads to the conclusion that linearization of $\exp[\tau'_{ij}(r)]$ must be less drastic than the similar linearizations occurring in PY and PYA, the reason being that $\tau'_{ij}(r)$ is comparatively small because now also the leading term of $h_{ij}(r)$ is almost cancelled out *as well as* that of $c_{ij}(r)$ in eqn. (3.10). Whether the PYRL contains a more balanced pair of approximations and hence is superior to the HNC remains on open question until we have actually solved the integral equations and compared them with the exact results.

In a previous work on the hard-sphere Coulombic system (RPM), one of us has described a solution method for the HNC equation.²³ The method is based on the traditional iteration technique,²⁷ but with the new feature of making maximum use of the analytic solution of the generalized MSA (GMSA) for this model.²⁸ The linear combinations (3.12a) and (3.12b), which in the

$$c_D(r) = \frac{1}{2}[c_{11}(r) - c_{12}(r)] \quad (3.12a)$$

$$c_S(r) = \frac{1}{2}[c_{11}(r) + c_{12}(r)] \quad (3.12b)$$

GMSA for the RPM and RPMY are approximated by eqns. (3.13a) and (3.13b) are the key elements in initiating the iteration process. In the present case, we have actually used the expression (3.13c) instead

$$c_D^{\text{GMSA}}(r) = -\beta u_D(r) + K_D \exp(-z_D r)/r \quad (3.13a)$$

$$c_S^{\text{GMSA}}(r) = K_S \exp(-z_S r)/r; \quad r > R \quad (3.13b)$$

$$c_D^{\text{MSA}}(r) = -\beta u_D(r) \quad (3.13c)$$

of (3.13a) because of the somewhat simpler solution for the initial set of correlation functions. The two remaining adjustable parameters, K_S and z_S , must be given values that yield a set of initial correlation functions that assures optimal convergence and accuracy of the iteration process. The solution method is otherwise as described by Larsen.²³

Results for the thermodynamic properties obtained with the HNC and PYRL equations are given in Table 1, and correlation functions are shown graphically in Section 6.

4. MONTE CARLO CALCULATIONS

The MC-calculations were carried out with a system containing 216 ions, 108 of each kind, in a cubic cell with periodic boundary conditions. Spherical cut-off at a distance r_c was used, and energy contributions from pairs with a larger interionic distance were neglected.

Our criteria for the choice of z and r_c was that $u(r_c)$ divided by $u(R)$ should be $\leq 1.0 \times 10^{-5}$. For practical reasons r_c was set to be $\leq L/2$, where L is the length of the cubic cell. From these criteria the z -values listed in Table 1 were chosen, with $r_c = L/2$ at the five highest densities, and with $r_c/R = 10$ at the ten lowest densities.

The usual Metropolis sampling²⁹ was employed. At low densities, this sampling method is inefficient because relatively small "pockets" of the phase space contribute significantly to the canonical means. When a configuration in one such pocket is accepted, many trial configurations may be required in order to escape the pocket, and this situation may lead to a practical ergodicity problem.^{30,31} The real-system analogue is the tendency to form ion pairs and larger clusters, which may indeed be observed also in the computer model.¹¹ Unless the system really is non-ergodic, however, the statistical noise can be reduced by prolonging the computations or bias the sampling.⁵ We have chosen to carry out some very long runs (in some cases 4×10^6 equilibrium configurations) in order to reduce the noise to an acceptable level and obtain the necessary material for a statistical analysis of our results.

Uncertainties in the computed results can be estimated from the scatter of subaverages based on consecutive small parts of the Markov chain.³⁰ One has to ensure that the subaverages are statistically independent in order to estimate the "within run" uncertainties from the usual normal-distribution formula.

Because of the increasing fluctuations as the system gets more dilute, we had to generate an increasing number of configurations to get satisfactory accuracy. For the six highest densities, $8 \times 10^5 - 10 \times 10^5$ equilibrium-configurations were generated, for the nine lowest densities, 4×10^6 equilibrium-configurations were generated, and at least $3 \times 10^5 - 5.5 \times 10^5$ configurations were rejected in each run prior to equilibrium.

A favourable acceptance ratio is about 50%, and by adjusting the maximum displacement of the ions this ratio was obtained for the seven highest densities. For the lowest densities, the acceptance ratios increased from 50 to 99.5% with decreasing density, fairly independently of the maximum displacement.

Numerical results for U/NkT are given in Table 1. The numerical results for the osmotic coefficient, PV/NkT , are given in Table 2. The results for the rdf's are given in Section 6.

5. THERMODYNAMIC PROPERTIES

Numerical results for the internal energy obtained from Monte Carlo calculations, the MSA, TF2A, TF2AUB₂, EXP, HNC and PYRL approximation are given in Table 1. The values for ρ^* and β^* were chosen from a range corresponding to that of aqueous solutions of 2-2 electrolytes from 0.0001 M up to 3 M. Specifically, the values for ρ^* are close or equal to those used in earlier investigations of the RPM,³² whereas β^* -values have been determined from the "contact" condition for the apparent correspondence between the RPM and the RPMY.⁶ This "contact" condition is based on the value of the chain sum at contact between two ions, $C(R+)$, and the requirement is that $C(R+)$ for the RPMY equals that of the RPM at the same number density. If the value of z is given, this will uniquely determine a set of corresponding values of β^* for the RPMY and RPM as discussed in our earlier paper.⁶ In the present case, we have determined β^* -values for the RPMY corresponding to the value 6.8116 for the RPM used in previous investigations.^{14,32} The z -values were chosen according to the desired range of the potential for use in MC calculations, as described in Section 4.

The uncertainties in the MC results are given as three standard deviations on the basis of the variance-within-runs.³⁰ Subaverages over consecutive parts of p configurations of the Markov chain were considered independent if $10^5 < p < 4$

$\times 10^5$ for the 4×10^6 configuration runs and $p=5 \times 10^4$ for the shorter runs. The estimated variance in the average energy was not found to depend on ρ in these intervals.

Unlike the situation for the RPM, there is no question about methodological problems due to the energy summation method in the present MC results. The correspondence between the RPMY and RPM is questionable, of course, and we shall return to this in a subsequent paper. For the time being, we therefore consider the relation between the RPM and PRMY in a qualitative way only, and focus our attention on the validity of the various theories as applied to the RPMY.

The results for the MSA and TF2A confirm earlier findings⁶ that both approximations are rather poor for the RPMY, the TF2A being somewhat more accurate at higher densities. Both theories give, for instance, an energy about 50% too high at $c=0.06265$ M, whereas the MSA is about 12% and the TF2A about 2% too high at 3 M. At the lowest concentrations tabulated, both theories appear to be very poor, although they must be correct in the (Debye-Hückel) limit of zero concentration. By adding ΔB_2 the MSA and TF2A can be drastically improved at low densities and slightly at intermediate densities, whereas ΔB_2 is numerically unimportant in the energy at high concentrations.

The second ionic virial coefficient is contained in the EXP, HNC and PYRL, which are indeed in good agreement with the MC results at low densities. These theories also approach the low-density limit of the rdf, $g_{ij}(r) \rightarrow \exp[C_{ij}(r)]$, correctly. The EXP energy is much too low at high densities because it overestimates $g_{+-}(r)$ at $r \gtrsim R$, whereas both HNC and PYRL are quite accurate for all densities studied and well within the uncertainties of the MC results at high densities. The HNC and PYRL differ from the MC results by at most 9 and 13%, respectively, at intermediate densities. This is more than can be explained by uncertainties in the MC results, and may be related to the theories' inadequate representation of ion clusters, as discussed in a recent paper by Rossky *et al.*¹¹ We shall return to this question in Section 6.

The PYRL is of the same overall accuracy as the HNC, and the results at high concentrations indicate that it may actually be superior at higher densities. Some preliminary results for $\rho^*=0.669$ show that the PYRL energy is 0.3, 1.9 and 2.3% too high at $(\beta^*, z) = (1.4191, 1.5075), (3.5476, 3)$ and

(5.3197, 4) respectively, when compared to MC results.⁶ The HNC energy is 3.6, 4.7 and 3.8% too high, respectively. The PYRL is probably also superior to Allnatt's version of the PY equation at high densities, where the PYA tends to the MSA. We have solved the PYA for one state only, $c=3M$, corresponding to the first line of Table 1. The PYA energy was determined to $U/NkT = -0.936$, which is already quite close to the MSA result.

This impression of the accuracy of the various theories is confirmed by the computed osmotic coefficients. Of most interest are the HNC and PYRL, which show a striking similarity, and are also very close to the MC results. The difference MC – integral equation osmotic coefficients is 2–3% at the two highest densities and less at the lower densities. The MC results are quite uncertain at the lowest densities because the extrapolation of $g_{+-}(r)$ to $r=R+$ is associated with large uncertainties there.

A check on the thermodynamic self-consistency of the theories is of interest because it is often used as a validity-test where computer-simulation results are lacking. The check is readily applied to the MSA, which is largely analytic, and some results for the excess osmotic coefficients are given in Table 2. By "excess" we here mean the difference between the osmotic coefficient for the RPMY and that of the hard-sphere model at the same number density ρ^* . The quantity PV/NkT for hard spheres was computed from the Carnahan-Starling equation,³³ for the MC and MSA energy-equation (MSA, E) results, and from the PY equation for the MSA pressure-equation (MSA, P) results. The MSA compressibility equation gives zero for $\Delta PV/NkT$. The MSA is found to lack self-consistency, as is well-known from work on the RPM. There does not seem to be any correlation between the self-consistency and the accuracy of the theory, however. For instance, at the highest density, MSA,E and MSA,P differ by 140% of the MC result, whereas the

MSA,E is 20% off the MC result. At the lowest density given in Table 2, the respective differences are 15 and 75%, in other words a better self-consistency, but a worse agreement with the exact result. This seems to be the trend throughout the table, although the uncertainties in the MC results become large, in per cent, for the low densities.

6. STRUCTURAL PROPERTIES

In this Section, we shall compare results for the radial distribution functions obtained by the MC calculations with those of the HNC, PYRL, MSA, EXP, LIN and SQ approximations. Some structural properties of the RPMY are then discussed in relation to those of two similar models, *viz.* the RPM and a charged soft-sphere model. In particular, we shall focus on the different theories' prediction of ionic association into triplets.

The rdf's between like ions for five different states are shown in Fig. 1a. Note that $g_{++}(r) \equiv g_{--}(r)$ for the RPMY. The curves are labelled with the approximate concentrations they refer to in order to facilitate comparison with results for other electrolyte solution models. The exact specification of each state is given in Table 1. The rdf's between unlike ions for three states are shown in Fig. 1b.

Excellent agreement is found between MC, HNC and PYRL for the highest and lowest concentrations. The EXP approximation also agrees with MC at the lowest concentration. The HNC and PYRL are fairly accurate at intermediate concentrations, whereas the MSA, LIN and SQ are rather poor over the entire concentration range.

MSA and LIN are indistinguishable at the scale used because $g^{\text{HS}}(r)$ is very close to unity, except at 3 M. Both approximations give negative values of $g_{++}(r)$ at $r \gtrsim R$, which is an unphysical situation since the rdf's represent probability densities. This flaw, which occurs in some thermodynamic states, is well-known from studies on the RPM.¹⁸ The poor accuracy of MSA and LIN for small r is not surprising since $|C(r)|$ becomes quite large. A linear approximation to $\exp[C(r)]$, which is the asymptotic form of $g(r)$ as $c \rightarrow 0$, is here a poor approximation. So is also a quadratic approximation, hence the drastic overestimation of $g_{++}^{\text{SQ}}(r)$ for $r \gtrsim R$. We note that both $g_{++}(r)$ and $g_{+-}(r)$ are underestimated in the MSA, which explains the superiority of the MSA,E results given in Table 2 as compared to the MSA,P results because the MSA,E depends only on the

Table 2. Excess osmotic coefficient for the RPMY.

ρ^*	β^*	z	$-\Delta PV/NkT$		
			MC	MSA,E	MSA,P
2.685×10^{-1}	2.2388	2	0.45	0.356	0.993
3.549×10^{-2}	3.7585	1	0.34	0.327	0.619
5.590×10^{-3}	4.5858	1	0.19	0.142	0.246
4.461×10^{-4}	5.7948	1	0.10	0.023	0.038

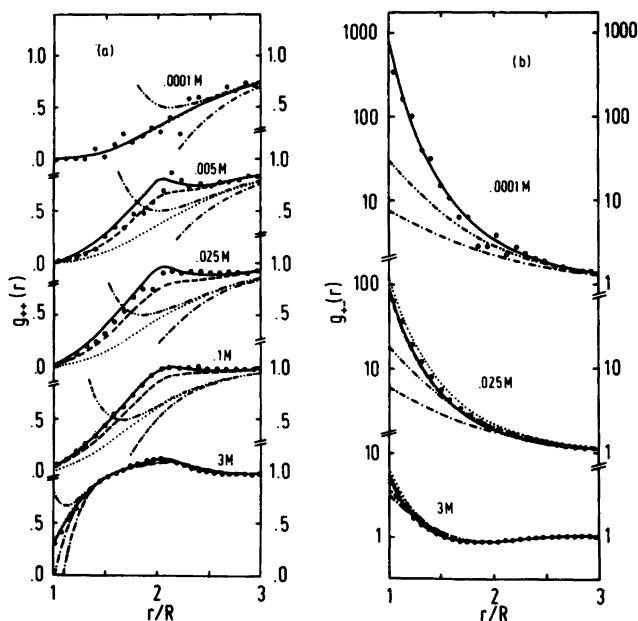


Fig. 1. Radial distribution functions $g_{++}(r)$, (a), and $g_{+-}(r)$, (b), for the RPMY corresponding to aqueous solutions of 2-2 electrolytes at 25 °C. The curves show MC (●), HNC (—), PYRL (---), MSA (-·-·-), LIN (- - - - -), SQ (- · - · -), and EXP (····) results as functions of reduced distance between centers of the hard spheres. The given concentrations are only approximate, exact specifications of the thermodynamic states are given in Table 1.

difference between $g_{++}(r)$ and $g_{+-}(r)$ whereas MSA,P also depends heavily on their sum.

In terms of an ionic virial expansion of $g(r)$, the large difference between MSA and EXP may be attributed to the fact that EXP contains the second ionic virial coefficient, but the MSA (or LIN or SQ) does not. This also explains the high accuracy of EXP at 0.0001 M. At higher concentrations, however, the EXP becomes rather poor, which we take as an indication of the importance of the third and higher-order virial coefficients. The HNC, which includes the complete third ionic virial coefficient, and the PYRL, which has got important contributions from it, are indeed more accurate at these intermediate concentrations. The differences occur mainly in $g_{++}(r)$ at $r \approx 2R$, and we note that the contact values of $g_{++}(r)$ and $g_{+-}(r)$ are quite accurate in the EXP, HNC and PYRL. If the EXP is equally accurate for the contact values of the RPM rdf's, our "contact" condition for the correspondence between RPM and RPMY states is certainly numerically accurate in addition to being justified on formal grounds.⁶

The high contact values of $g_{+-}(r)$ are typical for ion-pair formation. This feature is well-known from experimental and theoretical studies of electrolyte solutions, and must also be expected for the RPMY since it is determined mainly by the interactions at short range. The relatively high values of $g_{++}(r)$ at $r \approx 2R$ and intermediate concentrations reflect a tendency of triplet-ion formation. This has received less attention since the classic works of Fouss and Kraus,³⁴ but may play an important role in *e.g.* electronic exchange reactions.³⁵ The importance of $+-+$ and $-+-$ aggregates in the RPM was discussed by Friedman and Larsen on the basis of HNC calculations.¹⁰ Rosky *et al.* conclude in a recent paper that the HNC tends to overestimate $g_{++}(r)$ for a similar charged soft-sphere model in this region.¹¹ In particular, they carried out MC calculations that show no peak in $g_{++}^{\text{MC}}(r)$ beyond statistical noise at 0.005 M, whereas their $g_{++}^{\text{HNC}}(r)$ has a distinct peak at $r \approx 2R$, like that found for the RPM. Correcting the HNC by including the simplest bridge diagram, Rosky *et al.* found that the new equation, which they called the BHNC

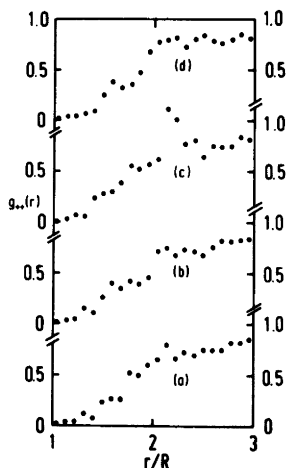


Fig. 2. Monte Carlo results for $g_{++}(r)$ at 0.005 M. The 4×10^6 configuration run has been divided into four consecutive parts in sequence a–b–c–d. Each curve shows a subaverage over 10^6 configurations.

equation, does not give this particular peak, in closer agreement with their MC results and with results from the PYA equation. Their conclusion was that the HNC equation greatly exaggerates the importance of triplets and large aggregates.

Our work on the RPMY shows that for this model, the HNC hardly seems to overestimate the number of triplets. As a matter of fact, the MC results for 0.005 M do show a peak in $g_{++}(r)$ at

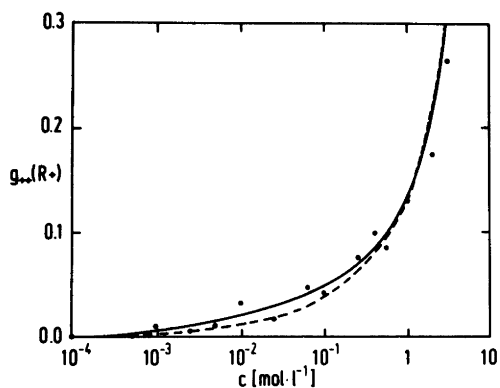


Fig. 3. Contact values of $g_{++}(r)$ as function of concentration c . The curves show MC (●), HNC (—), and PYRL (---) results for the RPMY corresponding to aqueous solutions of 2–2 electrolytes at 25 °C.

$r \approx 2.3R$ of the same height as that found in $g_{++}^{\text{HNC}}(r)$, but slightly shifted to larger r . At 0.025 M there does not seem to be a peak, but a shoulder in $g_{++}^{\text{MC}}(r)$ at $r \approx 2R$. The statistical noise level is acceptable at 0.025 M, but quite high at 0.005 M.

The apparent difference between our conclusion and that of Rosky *et al.* led us to analyze the MC results for 0.005 M in more detail. In Fig. 2, we have divided the run into four parts containing 10^6 configurations each. Only one of these parts (c) gives a distinct peak at $r \approx 2R$, and only about 5×10^4 configurations within this part actually contribute to the peak. It may seem like a triple-ion configuration is seldom hit during the MC sampling. But when a triple-ion is formed, it will persist long enough to count significantly in the average. In other words, there may be a practical ergodicity problem. The formation of triple ions is undoubtedly a real feature of the RPMY, but how important it will be in runs longer than 4×10^6 configurations remains an open question.

In light of our results, the conclusions drawn by Rosky *et al.* may seem doubtful. Their runs are relatively short, 6.4×10^5 configurations, whereas the peak in $g_{++}(r)$ at 0.005 M did not even show up until after 2×10^6 configurations. It should be kept in mind, however, that we compare two different models that may show different features in terms of triple-ion formation.

Both HNC and PYRL differ slightly from MC results for $g_{++}(r)$ and $g_{+-}(r)$ for $R < r < 2R$. This is also reflected in the internal energies listed in Table 1. The contact values of $g_{++}(r)$ are, however, in perfect agreement with the MC results. The concentration dependence of $g_{++}(R+)$ is shown in Fig. 3. The HNC results for charged soft spheres and the RPM show a maximum in $g_{++}(R)$ between 10^{-3} and 10^{-2} M. This has been interpreted in terms of triple-ion formation.¹⁰ MC and BHNC results for the soft-sphere model do not show this maximum, however.¹¹ Neither have we found it for the RPMY, as shown in Fig. 3. The close correspondence between RPM and RPMY on one hand and the HNC results for $g_{++}(R+)$ on the other seem to contradict each other, and the reason for this is not clear to us.

REFERENCES

1. Krogh-Moe, J., Østvold, T. and Førland, T. *Acta Chem. Scand.* 23 (1969) 2421.
2. Woodcock, L. V. and Singer, K. *Trans. Faraday Soc.* 67 (1971) 12.

3. Ewald, P. P. *Ann. Phys. Leipzig* 64 (1921) 253.
4. Evjen, H. M. *Phys. Rev.* 39 (1932) 675.
5. Valteau, J. P. and Whittington, S. G. In Berne, B. J., Ed., *Modern Theoretical Chemistry*, Plenum, New York 1977, Vol. 5.
6. Larsen, B. and Rogde, S. A. *J. Chem. Phys.* 72 (1980) 2578.
7. Hansen, J. P. and McDonald, I. *Theory of Simple Liquids*, Academic, London 1976.
8. Triolo, R., Grigera, J. R. and Blum, L. *J. Phys. Chem.* 80 (1976) 1858.
9. Valteau, J. P. and Cohen, L. K. *J. Chem. Phys.* 72 (1980) 5935.
10. Friedman, H. L. and Larsen, B. *Pure Appl. Chem.* 51 (1979) 2147.
11. Rossky, P. J., Dudowicz, J. B., Tembe, B. L. and Friedman, H. L. *J. Chem. Phys.* 73 (1980) 3372.
12. Waisman, E. *J. Chem. Phys.* 59 (1973) 495.
13. Andersen, H. C. and Chandler, D. *J. Chem. Phys.* 57 (1972) 1918.
14. Larsen, B., Stell, G. and Wu, K. C. *J. Chem. Phys.* 67 (1977) 530.
15. Allnatt, A. R. *Mol. Phys.* 8 (1964) 533.
16. Stell, G. In Domb, C. and Green, M. S., Eds., *Phase Transitions and Critical Phenomena*, Academic, London 1976, Vol. 5B.
17. Wertheim, M. S. *Phys. Rev. Lett.* 10 (1963) 321.
18. Larsen, B. *Dr.techn. Thesis*, University of Trondheim, Trondheim 1979.
19. Friedman, H. L. *Ionic Solution Theory*, Wiley, New York 1962.
20. Sun, S. F. *Ph. D. Thesis*, SUNY at Stony Brook 1978.
21. Verlet, L. and Weis, J. J. *Mol. Phys.* 28 (1974) 665.
22. Morita, T. and Hiroike, K. *Prog. Theor. Phys.* 25 (1961) 537.
23. Larsen, B. *J. Chem. Phys.* 68 (1978) 4511.
24. Percus, J. K. and Yevick, G. J. *Phys. Rev.* 110 (1958) 1.
25. Rasaiah, J. C. and Friedman, H. L. *J. Chem. Phys.* 48 (1968) 2742.
26. Mayer, J. E. and Mayer, M. G. *Statistical Mechanics*, Wiley, New York 1940.
27. Watts, R. O. In Singer, K., Ed., *Statistical Mechanics*, Chem. Soc., London 1973, Vol. 1.
28. Høye, J. S., Lebowitz, J. L. and Stell, G. *J. Chem. Phys.* 61 (1974) 3253.
29. Metropolis, M., Rosenbluth, A. W., Rosenbluth, M. N., Teller, A. N. and Teller, E. *J. Chem. Phys.* 21 (1953) 1087.
30. Wood, W. W. In Temperley, H. N. V., Rowlinson, J. S. and Rushbrooke, G. S., Eds., *Physics of Simple Liquids*, North-Holland, Amsterdam 1968.
31. Larsen, B. and Rogde, S. A. *J. Chem. Phys.* 68 (1978) 1309.
32. Rasaiah, J. C. *J. Chem. Phys.* 56 (1972) 3071.
33. Carnahan, N. F. and Starling, K. E. *J. Chem. Phys.* 51 (1969) 635.
34. Fuoss, R. M. and Kraus, C. A. *J. Am. Chem. Soc.* 55 (1933) 2387.
35. Menashi, J., Reynolds, W. L. and Van Auken, G. *Inorg. Chem.* 4 (1965) 299.

Received November 17, 1980.